

# Correction Filter for Single Image Super-Resolution: Robustifying Off-the-Shelf Deep Super-Resolvers Supplementary Material

Shady Abu Hussein  
Tel Aviv University, Israel  
shadya@mail.tau.ac.il

Tom Tirer  
Tel Aviv University, Israel  
tomtirer@mail.tau.ac.il

Raja Giryes  
Tel Aviv University, Israel  
raja@tauex.tau.ac.il

## 1. Additional results for the non-blind setting

Additional visual results of the different methods in the non-blind setting (which are not included in the paper due to space limitation) are presented in Figures 2 and 3.

We also present in Figure 1, the results obtained by the DPSR method [6] (using its official implementation code). It can be seen that DPSR results have many artifacts. In fact, DPSR average PSNR as produced by its official code is lower by more than 10 dB than the other examined methods (SRMD [5], ZSSR [3], DBPN [2], proSR [4], RCAN [7], and our proposed approach). Therefore, it is not displayed in the tables in the paper.

## 2. Additional results for the blind setting

Additional visual results of the different methods in the blind setting (which are not included in the paper due to space limitation) are presented in Figures 4 and 5. Results for DIV2K testset are presented in Table 1 below.

Table 1: Blind super-resolution comparison on DIV2K [1]. Each cell displays PSNR [dB] (left) and SSIM (right).

	x2	x4
DBPN	29.186 / 0.828	25.642 / 0.733
DBPN + estimated correction	29.389 / 0.832	26.204 / 0.736
kernelGAN (claimed)	<b>30.363 / 0.867</b>	<b>26.810 / 0.7316</b>



Figure 1: DPSR [6] results for non-blind super-resolution of baboon and monarch images from Set14, for scale factor of 2 and Gaussian downsampling kernels. Left is with filter of std  $1.5/\sqrt{2}$ , and right is with filter of std  $2.5/\sqrt{2}$ .

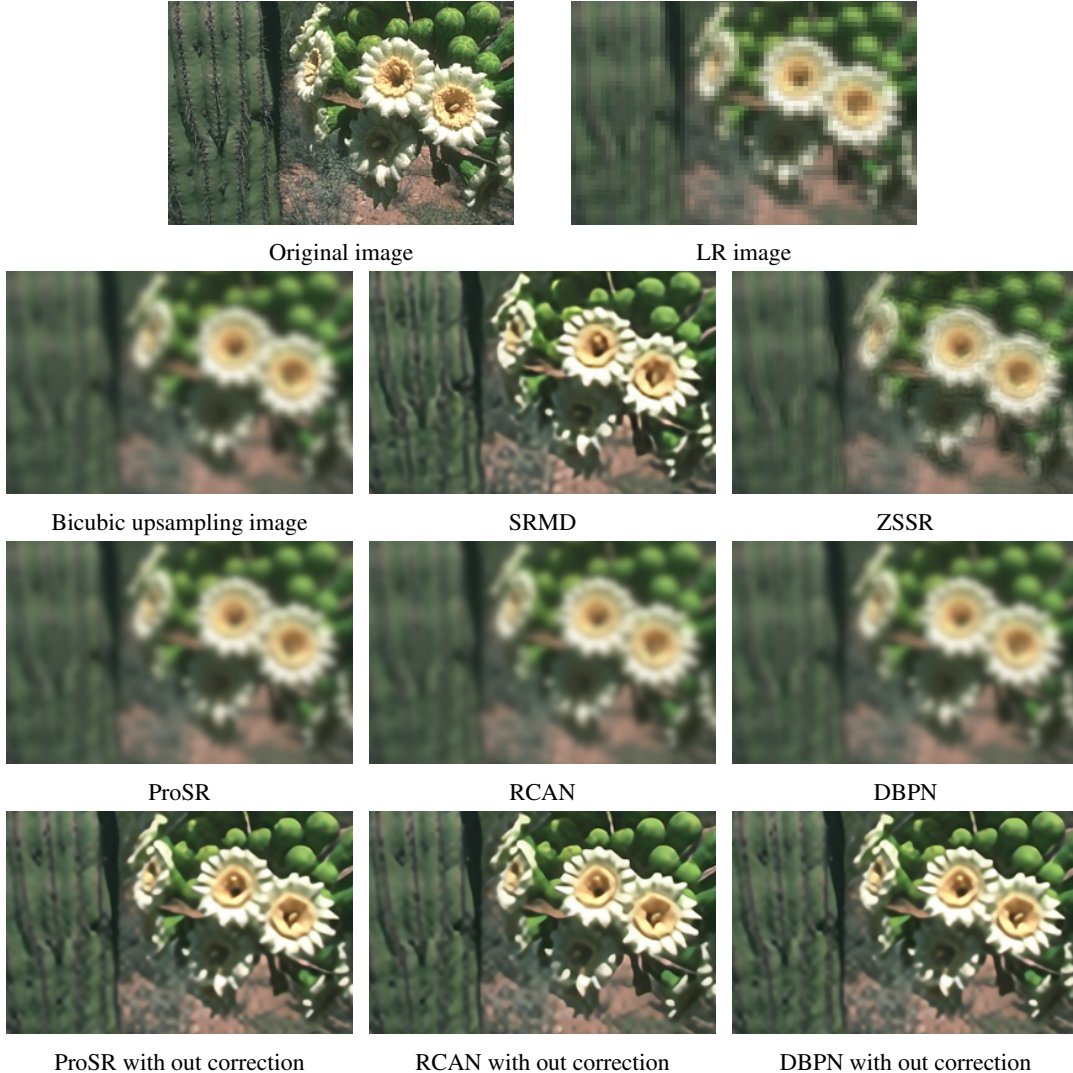


Figure 2: Non-blind super-resolution of image 19021 from BSD100, for scale factor 4 and Gaussian downsampling kernel with standard deviation  $4.5/\sqrt{2}$ .

### 3. The spectrums of sampling kernels

In Figure 6 we present the frequency spectrums of Gaussian kernels that are used in this work and two bicubic kernels, one for scale factor of 2 and one for scale factor of 4. In order to ease the presentation, the curves are plotted for the one-dimensional version of these kernels. Our experiments show that for super-resolution factor of 2 the proposed filter correction approach yields very good results for Gaussian sampling kernels of  $1.5/\sqrt{2}$  and  $2.5/\sqrt{2}$  (see Tables 1 and 2 in the main body of the paper), but not for  $3.5/\sqrt{2}$ . This behavior correlates with the recovery guarantees in Theorem 2. The theory essentially requires that the passband of the bicubic kernel (associated with relevant scale factor) is contained in the passband of the downscaling kernels. Indeed, it can be seen in Figure 6 that the passband of the bicubic kernel for scale factor 2 is contained in the passband of the Gaussian with  $1.5/\sqrt{2}$ , but extremely larger than the passband of the Gaussian with  $3.5/\sqrt{2}$ . On the other hand, for super-resolution factor of 4 we do get good results for Gaussian sampling kernel of  $3.5/\sqrt{2}$  (see Tables 1 and 2 in the main body of the paper). This is aligned with the fact that the bicubic kernel for scale factor 4 is much narrower in frequency domain than the bicubic kernel for scale factor 2, as shown in Figure 6.

We note that the deficiency of the correction filter approach for the setting with Gaussian kernel of  $\sigma = 3.5/\sqrt{2}$  and scale factor of 2 can be resolved by increasing the regularization parameter  $\epsilon$  used in (11), which helps compensating the null space

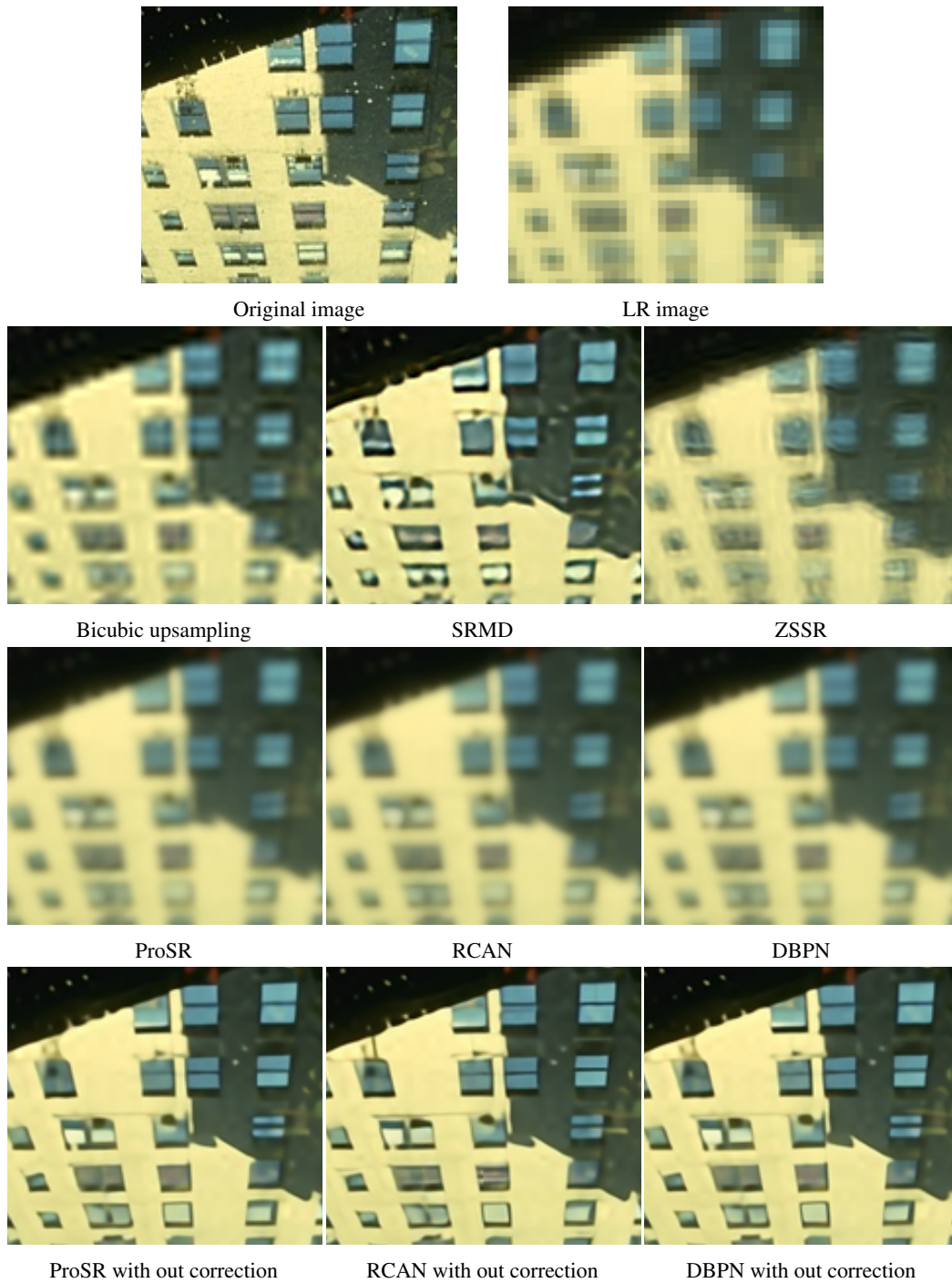


Figure 3: Non-blind super-resolution of image 148026 from BSD100, for scale factor 4 and Gaussian downsampling kernel with standard deviation  $3.5/\sqrt{2}$ .

in  $S^*\mathcal{R}$  and stabilizes its inverse. For example, plain application of DBPN on Set14 yields PSNR of 24.71 dB, and applying it after correction filter with  $\epsilon = 0$  yields PSNR of 10.34 dB. However, applying DBPN after correction filter with  $\epsilon = 10^{-5}$  yields PSNR of 28.67 dB.

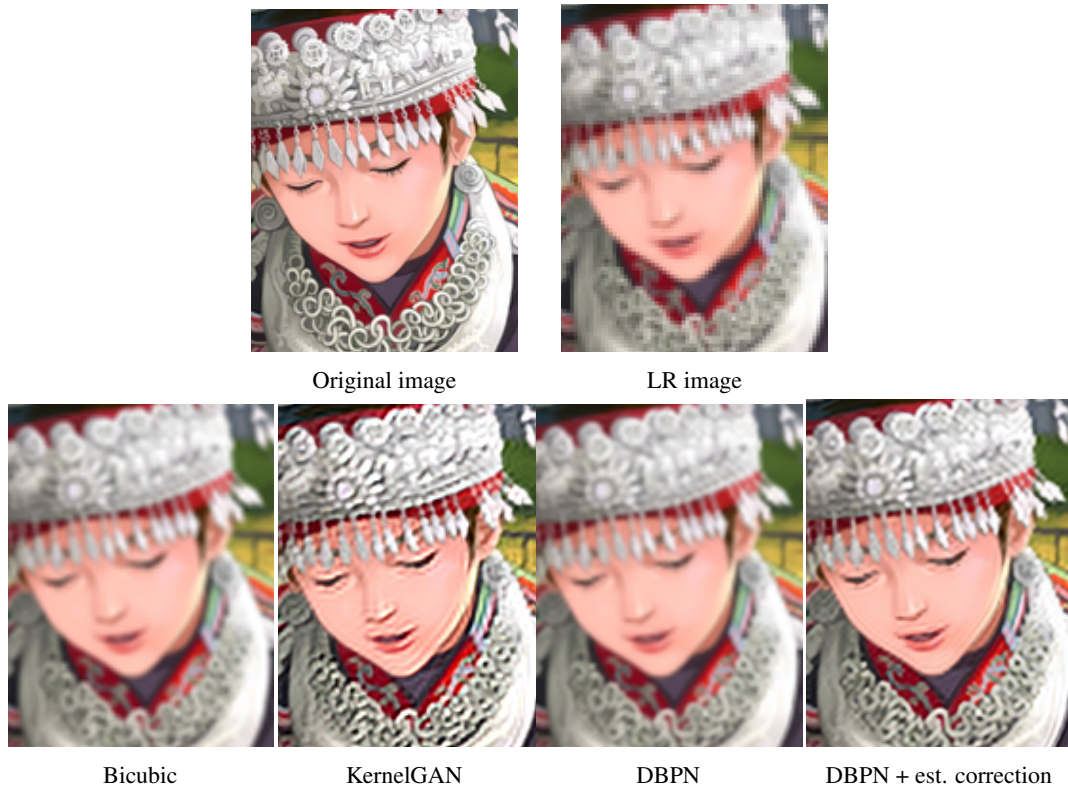


Figure 4: Blind super-resolution of *comic* image from Set14, for scale factor 2 and box downsampling kernel of width 4.

## References

- [1] Sefi Bell-Kligler, Assaf Shocher, and Michal Irani. Blind super-resolution kernel estimation using an internal-GAN. *Advances in Neural Information Processing Systems*, 2019. [1](#)
- [2] Muhammad Haris, Gregory Shakhnarovich, and Norimichi Ukita. Deep back-projection networks for super-resolution. In *Proceedings of the IEEE conference on computer vision and pattern recognition*, pages 1664–1673, 2018. [1](#)
- [3] Assaf Shocher, Nadav Cohen, and Michal Irani. “zero-shot” super-resolution using deep internal learning. In *Proceedings of the IEEE Conference on Computer Vision and Pattern Recognition*, pages 3118–3126, 2018. [1](#)
- [4] Yifan Wang, Federico Perazzi, Brian McWilliams, Alexander Sorkine-Hornung, Olga Sorkine-Hornung, and Christopher Schroers. A fully progressive approach to single-image super-resolution. In *Proceedings of the IEEE Conference on Computer Vision and Pattern Recognition Workshops*, pages 864–873, 2018. [1](#)
- [5] Kai Zhang, Wangmeng Zuo, and Lei Zhang. Learning a single convolutional super-resolution network for multiple degradations. In *Proceedings of the IEEE Conference on Computer Vision and Pattern Recognition*, pages 3262–3271, 2018. [1](#)
- [6] Kai Zhang, Wangmeng Zuo, and Lei Zhang. Deep plug-and-play super-resolution for arbitrary blur kernels. In *Proceedings of the IEEE Conference on Computer Vision and Pattern Recognition*, pages 1671–1681, 2019. [1](#)
- [7] Yulun Zhang, Kunpeng Li, Kai Li, Lichen Wang, Bineng Zhong, and Yun Fu. Image super-resolution using very deep residual channel attention networks. In *Proceedings of the European Conference on Computer Vision (ECCV)*, pages 286–301, 2018. [1](#)

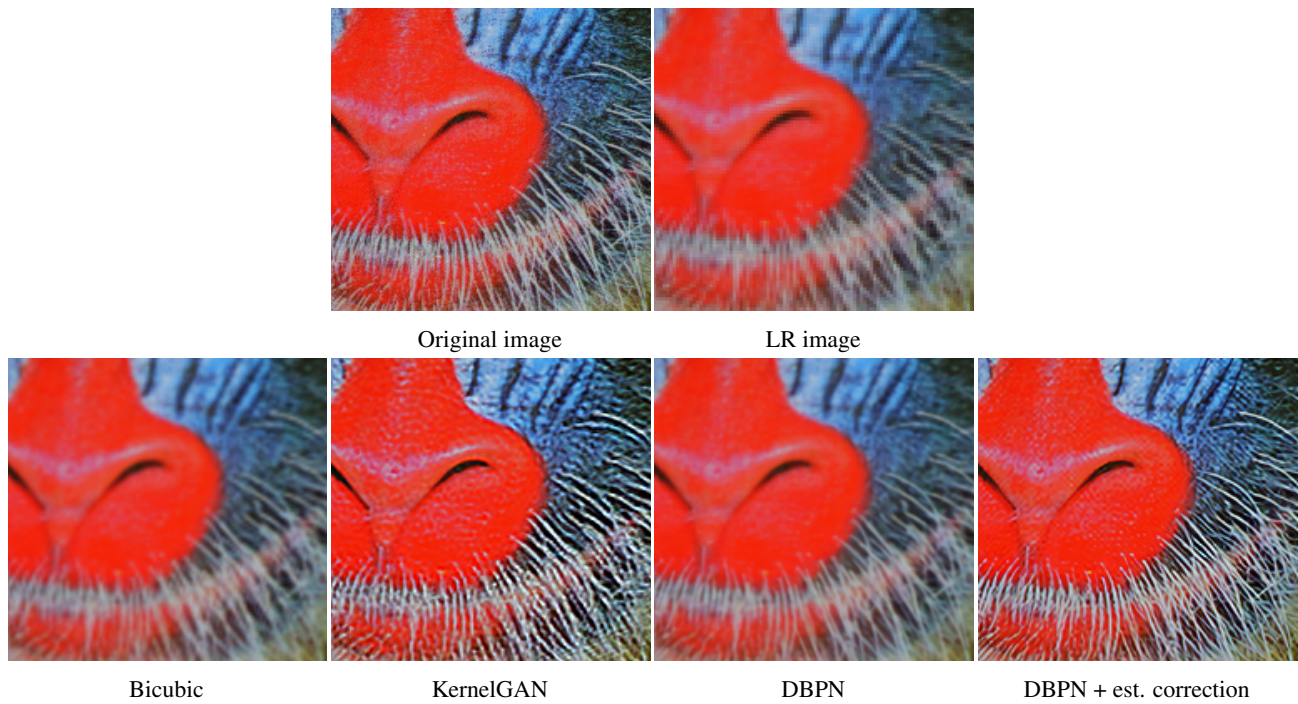


Figure 5: Blind super-resolution of *baboon* image from Set14, for scale factor of 2 and Gaussian downsampling kernel with standard deviation  $1.5/\sqrt{2}$ .

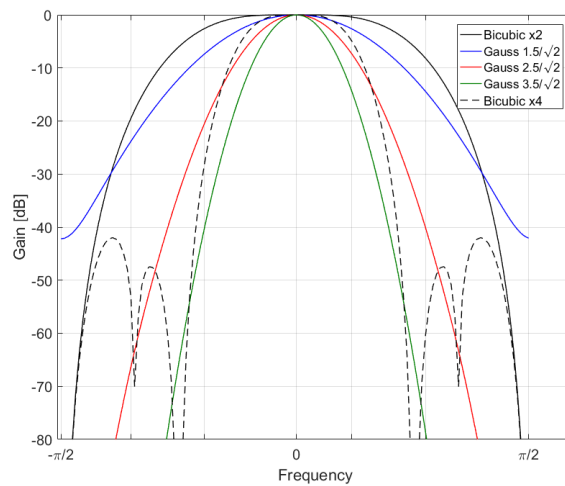


Figure 6: Frequency spectrums of different one-dimensional kernels.